

On the comparative cutting performance of nature inspired structured cutting tool in dry cutting of AISI/SAE 4140

Fatima, A. and Mativenga, P.T.

Author post-print (accepted) deposited in CURVE March 2016

Original citation & hyperlink:

Fatima, A. and Mativenga, P.T. (2015) On the comparative cutting performance of nature inspired structured cutting tool in dry cutting of AISI/SAE 4140. Proceedings of the Institution of Mechanical Engineers, Part B: Journal of Engineering Manufacture, volume In press.

<http://dx.doi.org/10.1177/0954405415617930>

Copyright © and Moral Rights are retained by the author(s) and/ or other copyright owners. A copy can be downloaded for personal non-commercial research or study, without prior permission or charge. This item cannot be reproduced or quoted extensively from without first obtaining permission in writing from the copyright holder(s). The content must not be changed in any way or sold commercially in any format or medium without the formal permission of the copyright holders.

This document is the author's post-print version, incorporating any revisions agreed during the peer-review process. Some differences between the published version and this version may remain and you are advised to consult the published version if you wish to cite from it.

CURVE is the Institutional Repository for Coventry University

<http://curve.coventry.ac.uk/open>

On the comparative cutting performance of nature inspired structured cutting tool in dry cutting of AISI/SAE 4140

Anis Fatima*, Paul T. Mativenga

School of Mechanical, Aerospace and Civil Engineering,
The University of Manchester, Manchester, M13 9PL, UK

*Corresponding author: anis.fatima@postgrad.manchester.ac.uk

Abstract

In this study femtosecond laser was used to create micro structures on the flank face of a cutting tool. For the first time, a nature inspired design (shape) of structure was created and explored. The inspiration for the nature inspired design was the ball python (snake). This is because these creatures have high resistance to damage, originating from skin surface design feature. This was the main reason in replicating its scale design on cutting tool surface. Orthogonal cutting test were performed on AISI/SAE 4140 at the cutting speeds of 283 and 628 [m/min](#) and a feed of 0.1 mm/rev to study the effects of structures shapes. Results showed that nature inspired design structures significantly reduced forces, temperature, compression ratio, contact length and power consumption. Characterisation of sticking and sliding contact was also made.

Keywords

Biomimetic, contact phenomenon, structured cutting tools, and surface structuring.

Introduction

Application of surface engineering at micro and nano level has gained significant attention over the recent years due to its benefits in tribological application and related areas (1). Examples include, surface structures in the form of small holes or grooves on the cylinder

liner honning that act as oil reservoirs, thus reducing wear. Micro-electromechanical systems (MEMS) devices that use surface structures for overcoming adhesion and friction. Mechanical seal that uses surface structures in a form of micro asperities that serves as micro hydrodynamic bearing for lubrication (2). One of the recent applications of engineering surfaces is an application of structured surfaces on the cutting tool for improving contact conditions at the tool-chip and tool workpiece contact zone. Research based on cutting tool structuring has shown promising results on reduced cutting forces (3-8), temperature (8-11), tool wear(5,8,9,12,13) and anti-adhesion properties (14). There are research that reports the optimal location (15) and positioning direction (3,6,7) for structures that are to be created on cutting tools. However, all the research available on cutting tool structuring is mainly focussed on rake face structuring with the exception of (8,12). Fatima et al (16) explore the flank face structuring in detail and recommended the benefits of flank face structuring.

Biomimetics is a relatively new technological field to manufacture the surfaces that have been used by nature for optimised functional use. There are many examples of successful biomimetic design that can be found in literature. Potential application of the biomimetic design extends from the context of material formation to the context of the coating/surface production. Investigation in biomimetic designs are currently applied to manufacturing processes (cutting, forming, grinding/abrasive), surfaces (self cleaning, liquid repellent and wear reducing), coating (friction reducing), precision engineering and metrology (sensing strategies). As noted, these concepts of application seem well suited to the application in the micro and nano regimes (17). However the novel engineering application of biomimetic design is in the field of surface engineering.

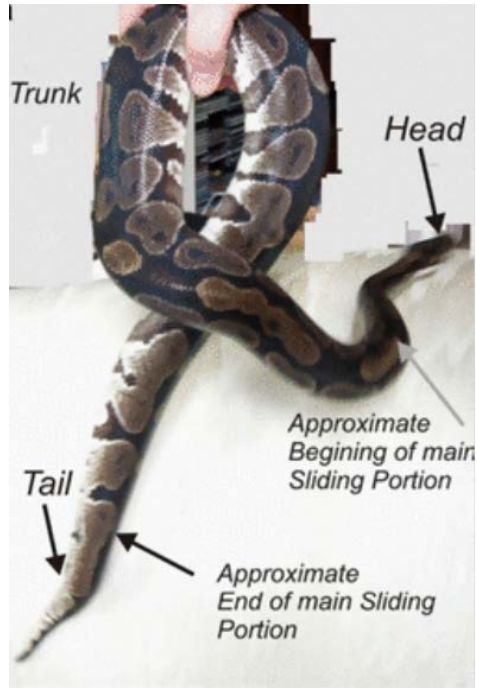
Recently, researchers have incorporated biomimetic characteristics into the tribological application. Jiang et al (1) showed that a synthesized cBN-TiN coating similar to the surface feature of *colocasia esculenta* (a plant), with nano-micro domes and pockets significantly

lowered friction coefficient by releasing a lubricants from the pockets, when put to a sliding test. Similar results were obtained when Wu et al (18) who prepared cBN-TiN coating having surface texture similar to lotus leaf.

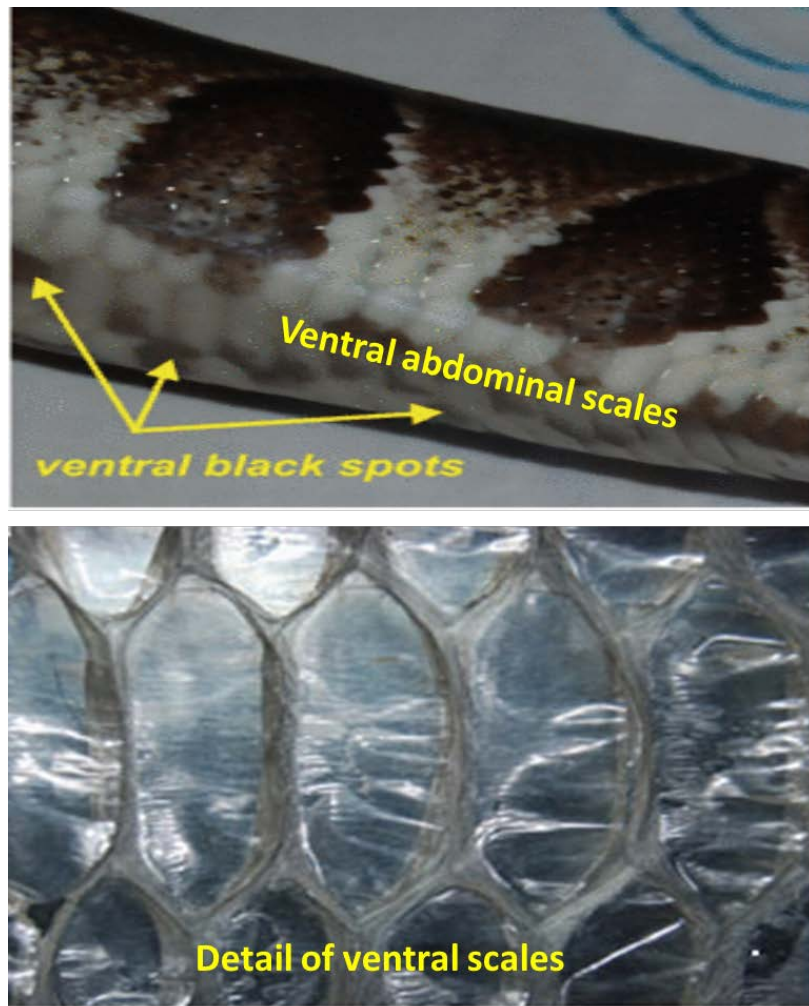
For reducing wear and thereby increasing the life span of agricultural tools, different plants (e.g. bamboo plant) and animals including the dung beetle, ground beetle, ant, centipede, earthworm, sandfish sink and the mole cricket have been recently investigated. The outer body surface of these animals and plants carriers unique geometrical features, regularly or randomly arranged with different shapes, sizes and numbers, which have proved to be favourable in reducing the abrasion wear (19). By using biotemplating (biomolding), where natural structured are copied, Han et al (20) replicated surfaces of sharkskin and other aquatics animals that has a broad prospective application in reducing the drag (friction). These biomimetic drag reducing surface which are light in weight and powerful in function are valuable in the manufacturing of submarine and aircraft with low load ability (20). In the past few years bio-inspired surface modification has brought a revolution in tribological applications.

With regards to this, in this study a consideration is given to the tool chip interface. A major concern in selecting bio inspired structures was to minimise friction, effective lubrication, save energy and reduced wear. As such, one of the species that serves as an analogue for these requirements is ball python skin; specifically scales (Figure 1) (21). It was selected because this creature, when sliding against various surfaces does not endure much damage. It is reported (21) that such an effect is stems from the asymmetric shape of the protrusion at the ridges of the skin scales. The presences of micron and nano sized fibril structures modifies the friction and adhesion during locomotion due to the minimization of the contacting surfaces while maintaining optimal sliding performance. Ball python ventral skin scales, irrespective of their size are not straight; rather they contain deviation (curves) and

form a hexagonal pattern. Further, the curvature of the leading edge is larger than the trailing edge. This help the snake to aid in shifting weight (contact load) and hence the contact angle (contact area) upon sliding (21). Ball python skin has two principle layers: dermis and strata. Dermis is the deeper skin layers with rich supply of blood vessels and nerves while strata is closely pack cells forming the outer protecting coating. Strata have no blood supply but obtain its nourishment by the diffusion to and from dermis. The outermost dead skin cells of snake are constantly flaking off and the protective layer top-up from the below. When the skin below undergoes a final maturation, fluid is exuded and forms a thin layer, well retained in skin structure between the new and the old layer. This fluid between the two skin give milky appearance to a shedding skin and help reptile actively remove it. Topographical feature of ball python skin revealed functional requirement of quality lubrication and decrease contact conditions, and thus decreased friction and wear. Keeping discussion to the tool chip contact phenomenon in a machining, above two mention aspects of snake skin function were judge to correlate to the contact process in machining. Nature inspired structures performances is studied and compared with conventional shaped structures and unstructured cutting tool.



a) Ball Python



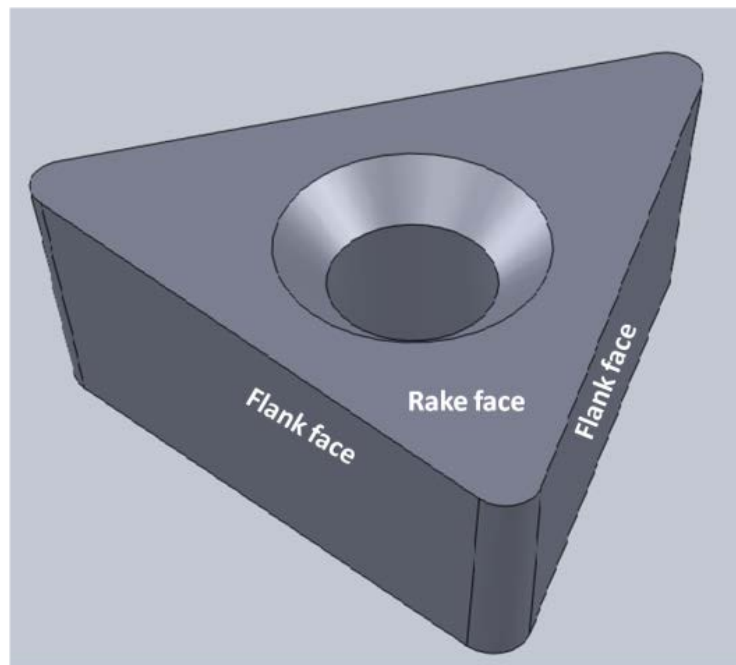
b) Snake scales detail

Figure 1 Biomimetic analogue for the non-conventional structures (21)

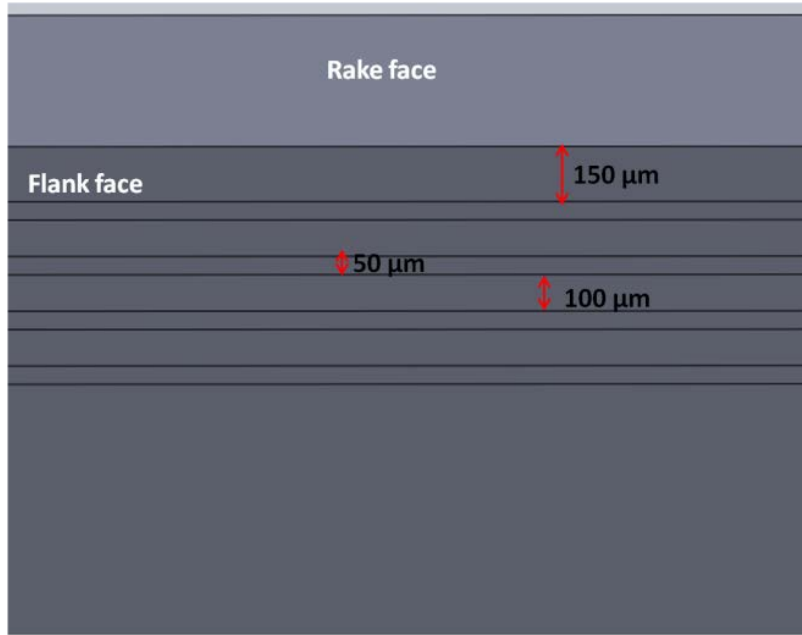
Experimental details

Conventional and non conventional structures were created on uncoated flat cemented carbide inserts (Sandvik TCMW 16T308 5015) as shown in Figure 2 and 3. The average cutting radius of insert was 28 μm . All dimensions were made to ± 5 mm. Ti: sapphire femto-second laser machining with the centre wavelength of 800nm, the repetition rate of 1 kHz and pulses of a width of 100fs was used to fabricate these structures. The average pulsed energy of 1 mJ was used. The energy stability was $\pm 12\%$ of the average value. The laser spot size was of 30 μm . These laser parameters were identified by Fatima et al (22) in a research study

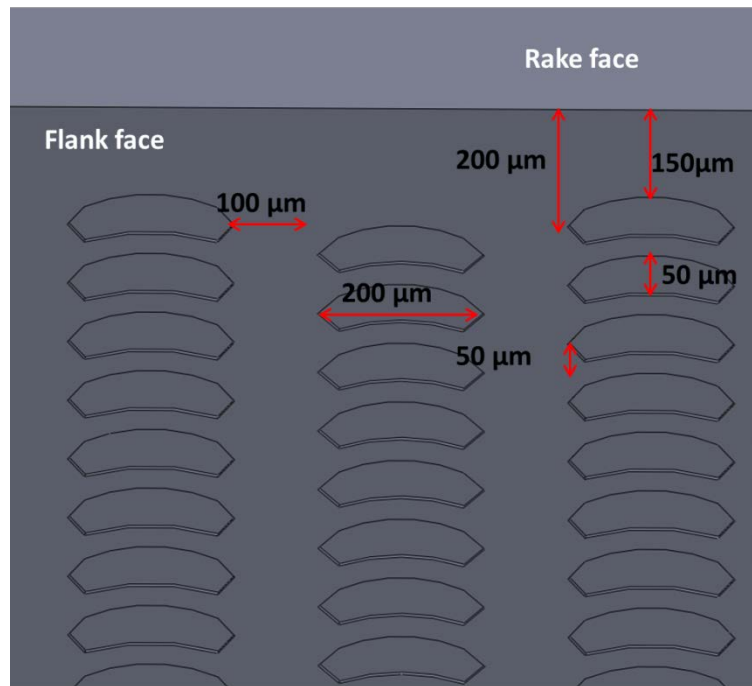
on femtosecond laser processing of carbide without compromising insert's surface integrity and mechanical properties. Cutting inserts were clamped in a fixture on a computer controlled translation stage. The stage was translated at the speed of 10 mm/s in front of a fixed laser beam. All experiments were performed in air (i.e. at ambient condition without cutting fluid) therefore all cutting inserts were washed for 10 min for the [removal of debris](#) in deionised water.



a) Conventional insert

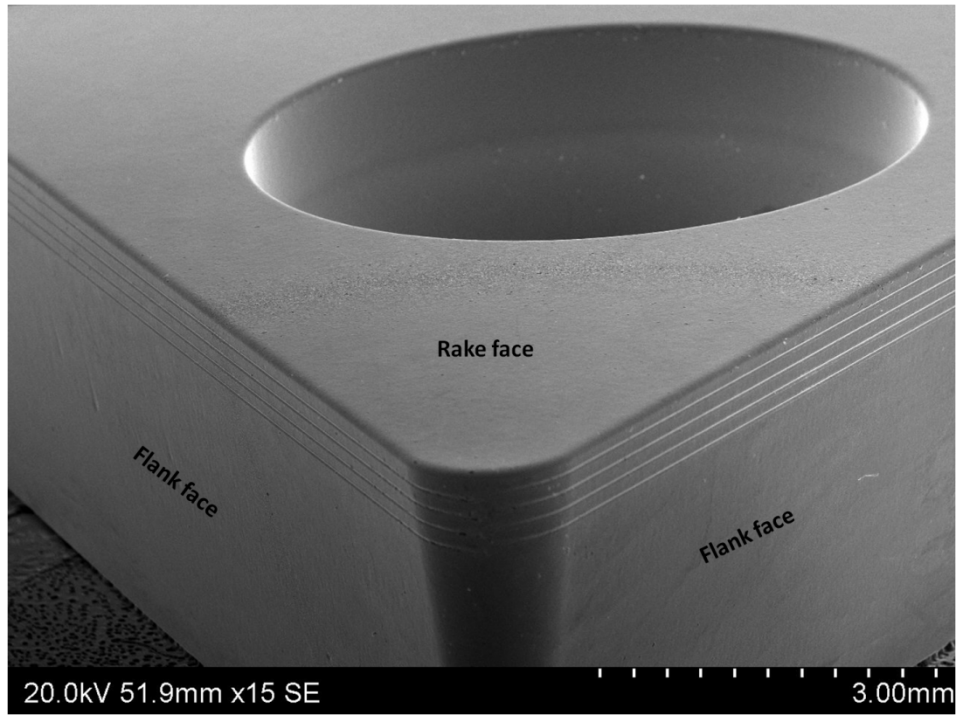


b) Conventional structures



c) Non conventional (Snake scale inspired) structures

Figure 2) a) Conventional insert, b) convectional structures and c) non-conventional structures



a)

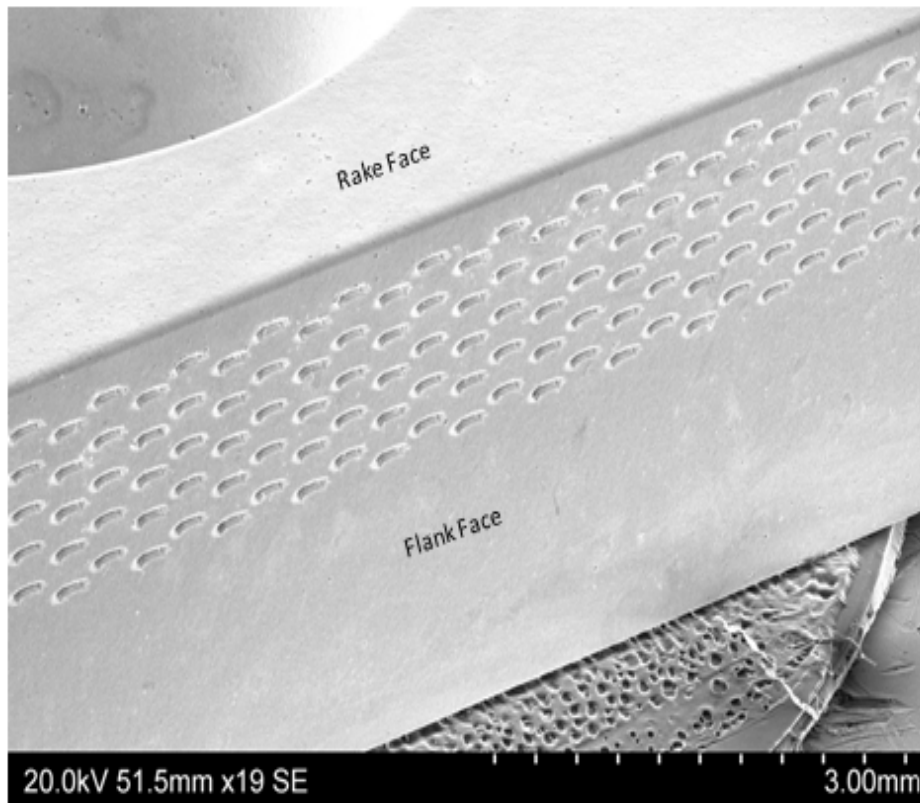


Figure 3 SME image of a) conventional and b) non conventional structures on cutting insert

Machining setup

Orthogonal cutting tests were performed on AISI 4140 plain carbon steel. AISI 4140 was selected as a work piece material because of its wide industrial use. The work material was in a form of tube with the outer diameter of 200 mm and a wall thickness of 2.5mm. Inserts were mounted on Sandvik STGCR 2020k-16 tool holder. It has zero rake angle and 7° clearance angle. The width of cut was fixed to the thickness of the tube, 2.5 mm and the feed rate was also fixed to 0.1 mm/rev. Cutting speeds of 283 and 628 m/min were selected to test the structures performance. As a lubricant; cutting compound, Trefolex, from Warren Bestobell was applied on the flank face of the cutting tool. All the experiments were repeated 3 times. Length of cut for each experiment was kept constant to 5 mm. Limitation of 5 mm length of cut (linear machining length) was justified in study conducted by Fatima et al (23). It was explained that the flank wear developed for machining 5 mm length falls within a very low range of values and thus it is not expected that it influence the rake angle and therefore the tool wear to affect the process. Another justification that was made was based on the stabilization of forces. It was argued that the time required for the full engagement of the tool cutting edge with the work piece is very rapid. During this phase the contact area and thus the wear happen to increase (so as the temperature) over this engagement and then remain reasonably constant. This is reflected by the stabilization of forces. In this regards the linear machining length of 5 mm is neither persistent nor significant for a flank were to affect the process.

Cutting forces were measured using piezoelectric KISTLER dynamometer type 9263. When the forces were stabilised, average value of forces were calculated from time domain force trend. Contact length was measured on worn inserts by measuring wear marks through scanning electron microscopy (SEM) images. Compression ratio was calculated by

measuring weight and geometry of produced chips. The temperature profile generated on tool rake face during machining, was captured by IR thermal image FLIR ThermoCAM® SC3000 camera. Temperature was recorded at a distance of 1 mm from cutting edge on the path of 1 mm on both sides away from the contact area. The camera was mounted at a distance of 0.4 m. ThermoCam Researcher software was used to study temperature profile from stored image data using Thermal emissivity of tool material of 0.48 at 700 °C. Thermal emissivity of tool material was established from furnace measurement.

Results and discussion

Temperature

Figure 3a shows a temperature profile at a cutting velocity of 283 m/min for conventional structured cutting insert. Whilst, Figure 3b shows the temperature distribution on the rake face of the cutting inserts. At the speed of 283 m/min highest temperature, 153 °C, was observed for unstructured cutting insert. At this cutting velocity temperature reduction of 12% and 65% was observed for conventional and non conventional structures, respectively. For the cutting velocity of 628 m/min, rake face temperature for unstructured cutting tool was 170 °C. Conventional structures show an increase of 9% in temperature than unstructured insert whereas, non conventional shows a reduction of 49% for the same cutting velocity, 628 m/min.

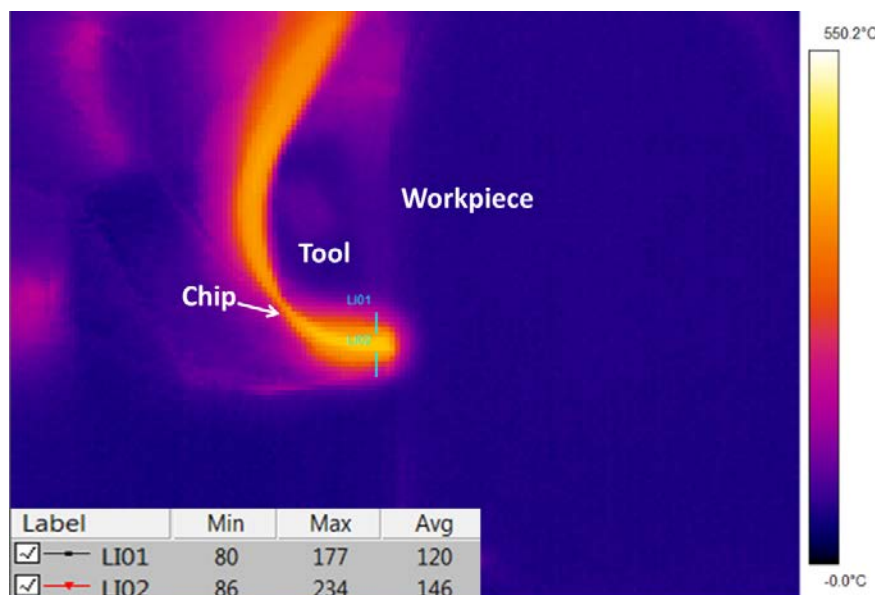


Figure 3a Temperature profile at cutting velocity of 283 m/min for conventional structured cutting insert

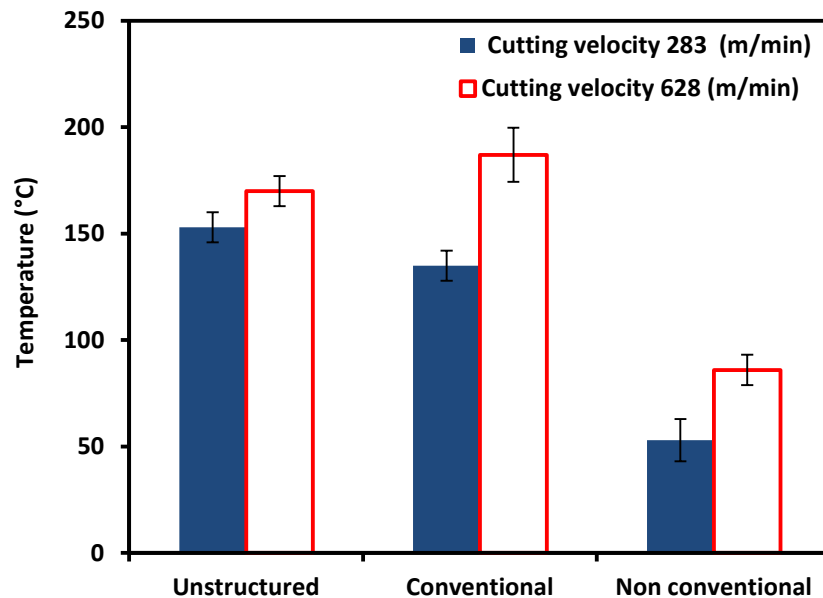


Figure 3b Rake face temperature

The reduction in temperature at high cutting velocity encountered may lead to the following explanation. There are several factors (ambient temperature, speed, applied load) that affect the energy losses at rubbing surfaces. Topography of the rubbing surfaces is one of them and is quite crucial as it affects the quality of lubrication (21). Therefore, fabricating structures resembling predetermined topography of snake skin scale have responded to the changes in rubbing condition at tool workpiece interface and have yielded predictable response in lowering temperature through effective lubrication.

Cutting forces

Average plot for the feed force and cutting force are represented in Figure 4a and b. For both the cutting velocities, conventional and non conventional structured cutting tool show reduction in feed and cutting forces. For the cutting speed of 283 m/min the reduction in feed

force associated with conventional and non-conventional was 3% and 6%, respectively. Whereas, for the cutting force the reduction was 4% for conventional structures and 8% for non conventional structures. However, at the cutting velocity of 628 m/min 4% reduction was observed in feed force for both conventional and non conventional structured tool. 13% and 16% cutting force reduction was obtained when conventional and non conventional structured tool was employed for machining at the cutting velocity of 628 m/min.

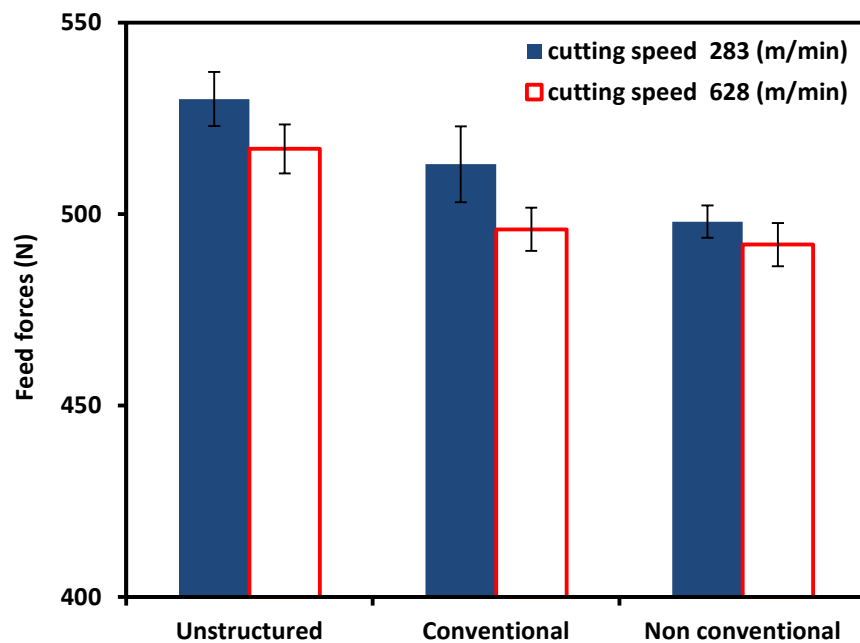


Figure 4a) Feed forces

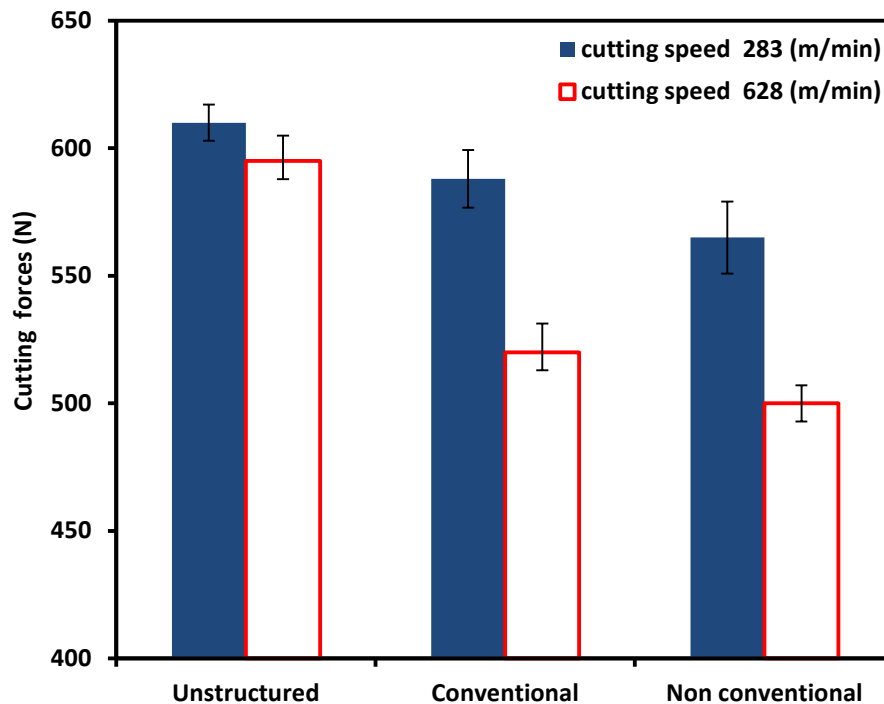


Figure 4b) Cutting forces

For zero degree rake angle feed forces are the reflection of friction forces on the rake face. Therefore, feed forces can be considered as a product of shear strength of the chip material and the contact area on the rake face. Conventional and non-conventional structured cutting tools have significantly reduced the contact length (Figure 5 and 6). This has decreased the friction force and hence the feed force (16). Whereas, cutting forces are the consequence of shearing and friction processes in metal cutting process.

Compression ratio

Figure 5 presents the variation of compression ratio for the unstructured, conventional and non conventional structured cutting tools for the speed of 283 and 628 m/min. Non conventional structured cutting tool yields lower compression ratio values for both cutting velocities than conventional and unstructured cutting tool, resulting in thinner chips. This can be attributed due to curve shape structures that aid in distributing chip load (one of the snake skin characteristics) and hence further decrease compression ratio Thinner chip reduce

contact length by promoting early chip curl and thus save energy (24). Information regarding rate of plastic deformation in deformation zone can be obtained by compression ratio. Also, It is established that increase in shear angle is conveyed by the decreased in compression ratio. Also, an increased shear angle designates a decreased shear plane. The work material is forced to deform in a small shear plane area resulting in high temperature in the vicinity of cutting plane. This increased in temperature decreases the yield strength of the material allowing ease cutting of the work material

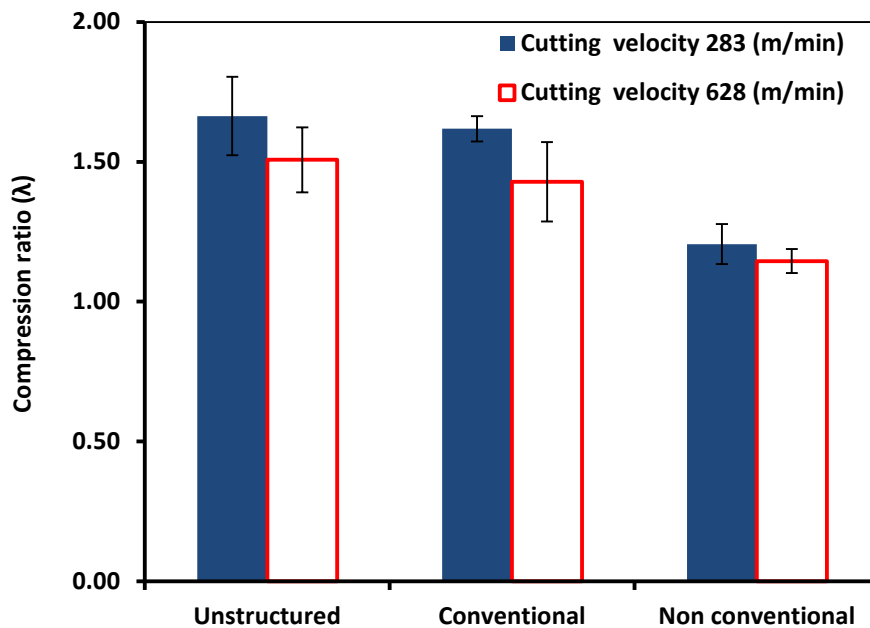


Figure 5) Compression ratio

Contact length

Figure 6 shows the average tool chip contact length for the selected cutting tools. It is evident from Figure 6 that the reduction in tool chip contact length is brought about by conventional and non conventional structured cutting tool. At both the cutting speed maximum reduction in tool chip contact length was brought by non conventional structured cutting tool which was 41% at 283 m/min and 13% at 628 m/min. Lower compression ratio values (Figure 5) represents decrease in a chip thickness due to nature inspired flank face structuring. Therefore, it can be viewed that tool flank face structuring has influenced the plastic flow of chip material and has facilitated the early chip curl. This is followed by the decrease in the contact length.

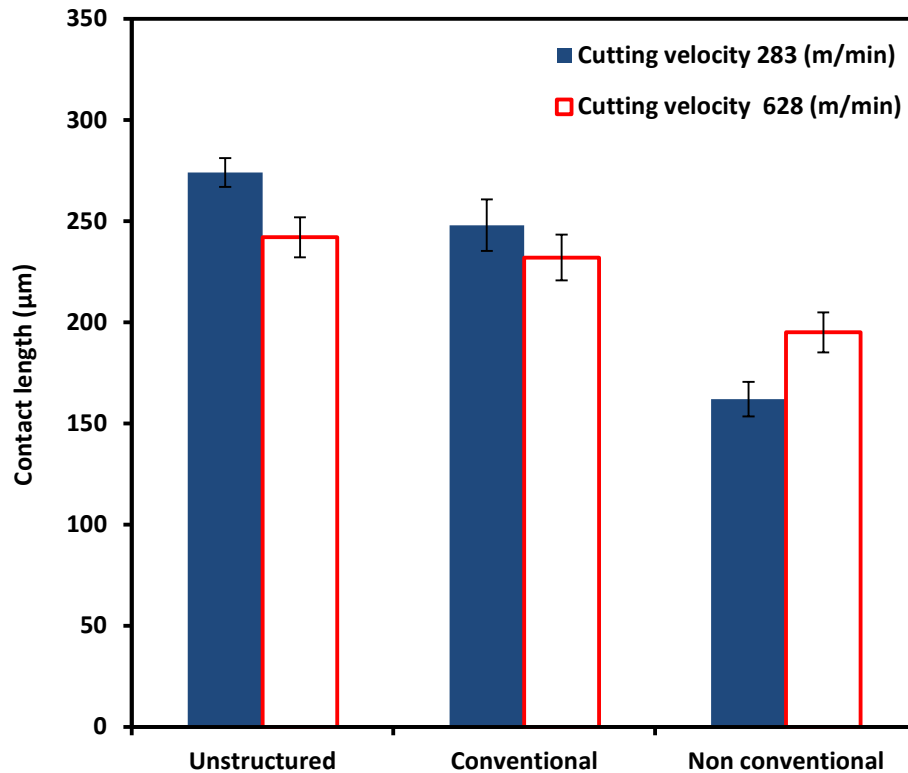


Figure 6) Tool chip contact length

Flank wear

Flank wear describes the gradual erosion of the portion of the tool which is in contact with the workpiece. It is an estimate to describe the expectancy of tool life. Figure 7 shows flank land wear for the cutting velocities of 283 and 628 m/min for the selected cutting tools. A decrease in the flank wear is observed for conventional and non conventional structured cutting tool than unstructured cutting tool at the speed of 283 m/min. However, non conventional structured cutting tool maintains ability to decrease wear even at higher cutting velocity of 628 m/min. This could be because of the low tool temperature due to predetermined structure shape for effective lubrication of non conventional structures.

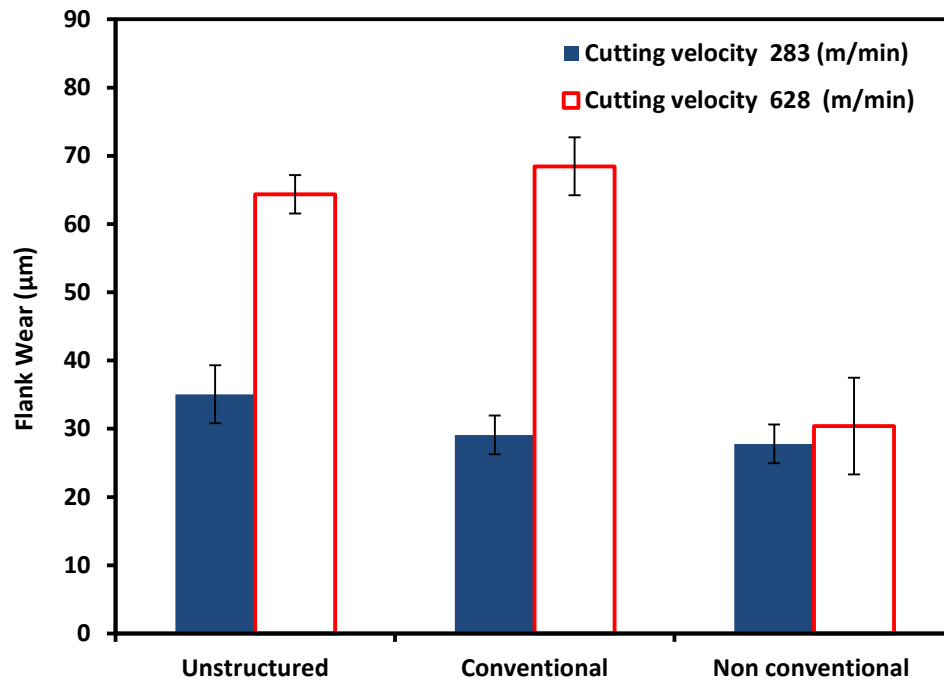


Figure 7) Flank land wear

Power

Reducing power consumption is based on the fact that less power is consumed during actual cutting incident. This is because as it is evidenced from literature, machine tool itself is the dominant power consumer rather than the actual chip formation process (25).

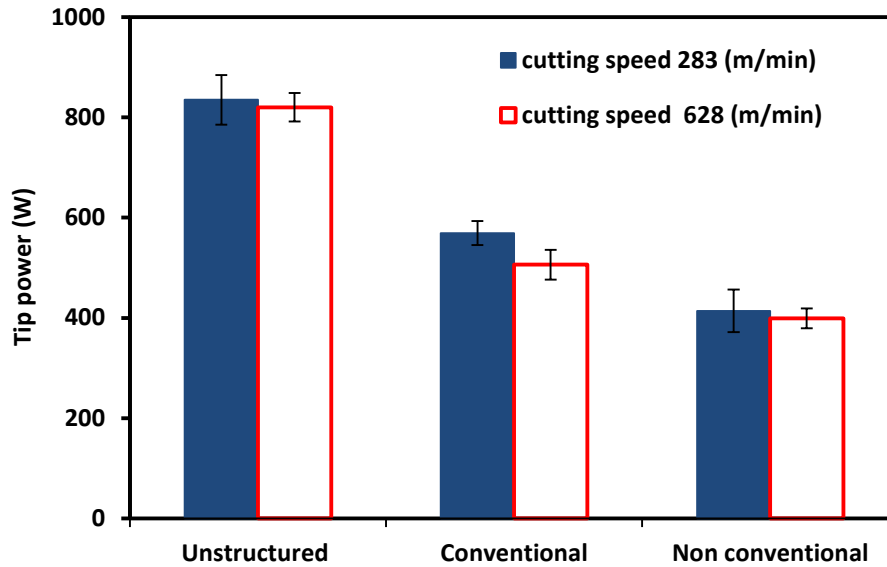


Figure 8) Power consumption

At the speed of 283 m/min power consumption for the conventional structured cutting tool was reduced by 32% whereas, for nonconventional cutting tool, 50% reduction was observed. Benefits of structuring were also observed for the cutting velocity of 628 m/min. Power reduction associated with the conventional and non conventional structured cutting tool was 38% and 51% than unstructured tool. From results it is established that on average, a further 14% reduction in power was observed when a cutting tool with non conventional structures on flank face was used for cutting. [Cutting power reduction is attributed due to the reduction in cutting forces.](#)

Sticking sliding contact

[Scanning electron microscope \(SEM\) fitted with Rontec energy dispersive spectroscopy \(EDX\) was used to analyse sticking and sliding conditions. This EDX system can detect various elements from boron to uranium. Iron transfer was quantified on tools rake face along tool chip contact length. It is established that Fe transfer supports the presences of sticking and sliding contact conditions on the rake face of cutting tool. High concentration of iron indicates the presences of sticking contact whereas low iron percentages support sliding contact \(26-28\). Figure 9a and b represents the corresponding iron weight percentage transfer for the cutting velocities of 283 and 628 m/min for the selected cutting tools. For the cutting](#)

speed of 283 m/min unstructured cutting tool develops an average of 30% of iron weight percentage transfer. For the conventional and non conventional structured cutting tool the average iron wt% transfer was reduced to 22% and 17% respectively. Further, high percentage of iron transfer was concentrated over 37% of contact length at cutting edge and represents the value of 53% of Fe wt%. This high concentration of iron transfer represents sticking contact over this length of contact length. High concentration of Fe wt% transfer was not observed for conventional and non-conventional structured cutting tool, representing only sliding contact prevailing at entire contact length at the cutting velocity of 283 m/min. At the cutting velocity of 628 m/min the average Fe wt% transfer of 56% was observed for unstructured cutting tool, whereas, conventional and non-conventional cutting tools develops Fe wt% transfer of 46% and 45% respectively. Moreover, high concentration of wt% transfer was concentrated at 80% of contact length in the case of unstructured cutting tool. Reduction of 20% and 30% was seen in the region of high concentration weight percentage of iron over the contact length. From the results presented above, it is revealed that morphing snake skin scales over the tool flank face has modified Fe adhesion over rake face of the cutting tool, reducing tool damage.

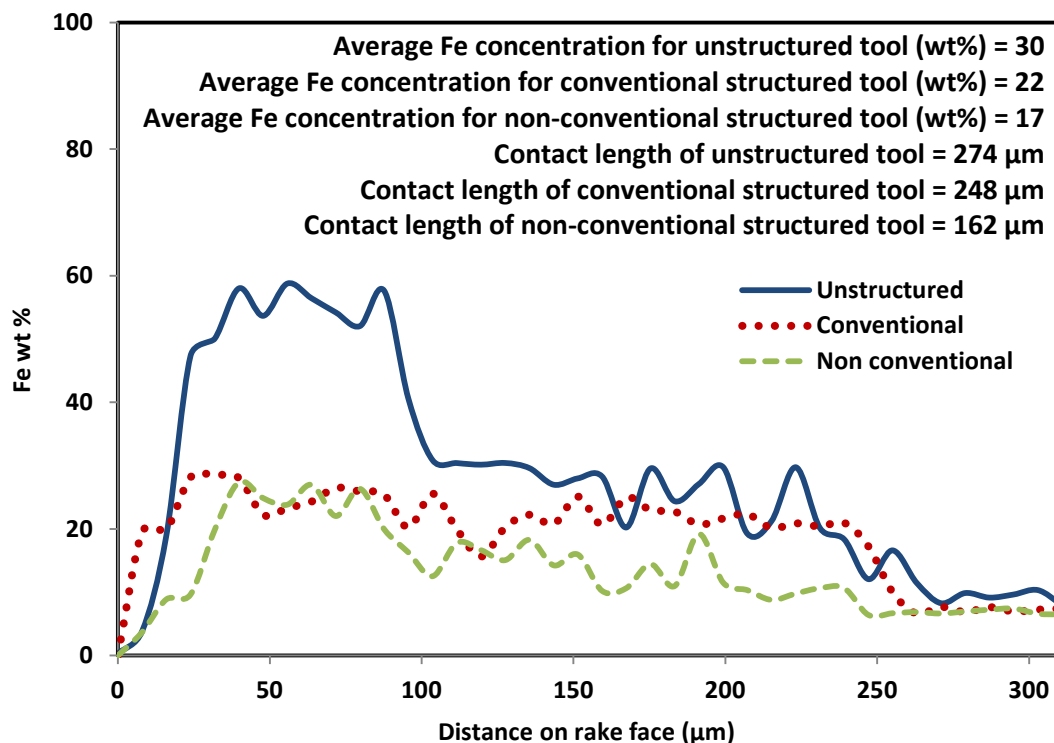


Figure 9a) Iron weight percentage transfer on tools rake face for cutting velocity of 283 m/min

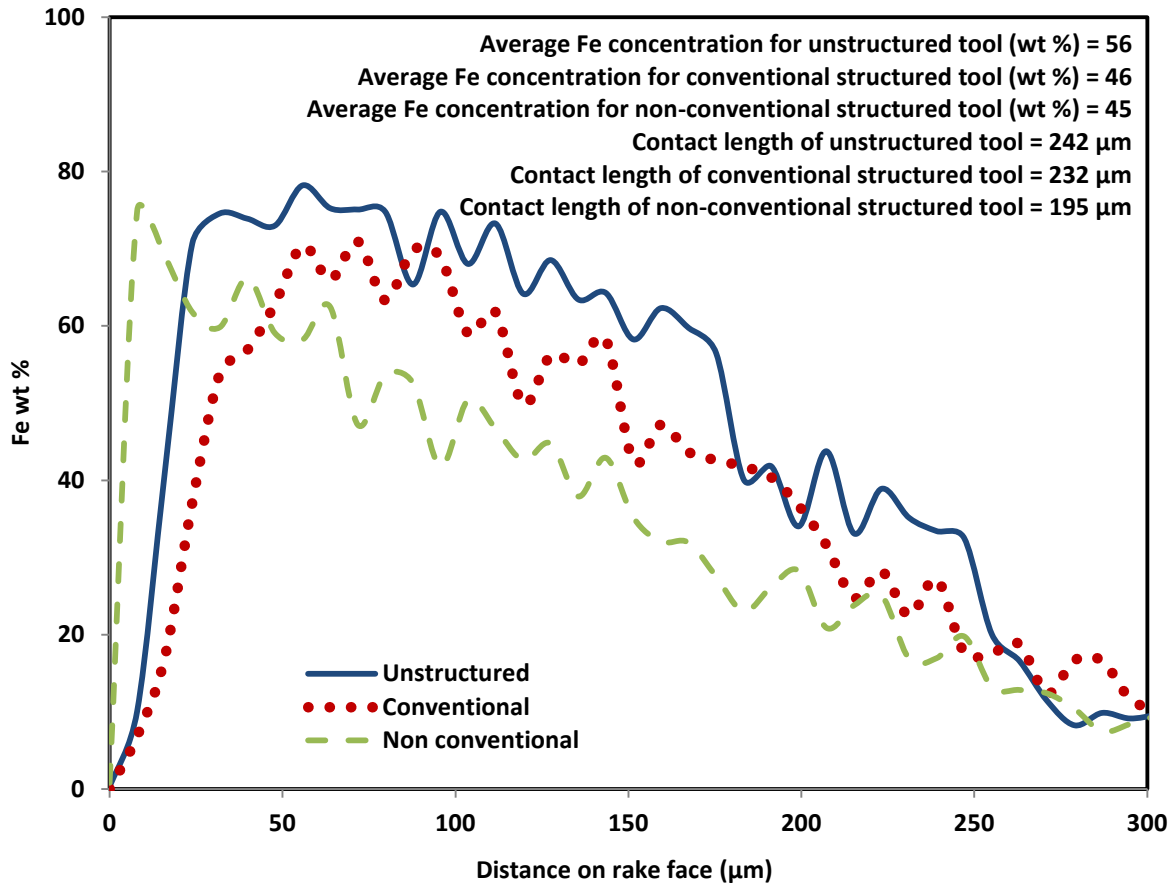


Figure 9b) Iron weight percentage transfer on tools takes face for cutting velocity of 628 m/min

Conclusions and future outlook

The main rationale to create predetermined geometric shaped structure on the cutting tool was to enhance the cutting performance and reduce wear. The flank face of the cutting tool was structured with shapes that resemble the scales on snake skin. Compared to unstructured and conventional structures some benefits in term of reduced cutting forces, tool wear, temperature, iron adhesion and compression ratio is delivered. However, to improve the optimal performance, it is suggested that the surface is required to maintain close morphology of the snake skin that is a micro protrusion above the surface in the form of curves and between two protrusions, a channel, which is supposed to retain lubricant. This pattern should be dense and cover the entire area of concern. The nature inspired design has retained the idea of wear resistance and cutting forces reduction. But clearly much work in terms of

fabrication method is required to copy the essential structure of the surface to make up analogies that can maintain its relation to friction and wear resistance up to optimum level. Also detail statistical analysis and contact phenomenon modelling can be beneficial in understanding mechanics of the process and the proof of concept. At present it is found that exact geometry control of ball python was not possible with the laser used. Further work should look at other high precision fabricating technologies that can control geometry at the micro scale.

- (1) Jiang W, Malshe AP, Wu JH. Bio-mimetic surface structuring of coating for tribological applications. *Surface and Coatings Technology* 2007;201(18):7889-7895.
- (2) Etsion I. Improving Tribological Performance of Mechanical Components by Laser Surface Texturing. *Tribology Letters* 2004;17(4):733-737.
- (3) Koshy P, Tovey J. Performance of electrical discharge textured cutting tools. *CIRP Annals - Manufacturing Technology* 2011;60(1):153-156.
- (4) Lei S, Devarajan S, Chang Z. A study of micropool lubricated cutting tool in machining of mild steel. *Journal of Materials Processing Technology* 2009;209(3):1612-1620.
- (5) Xing Y, Deng J, Zhao J, Zhang G, Zhang K. Cutting performance and wear mechanism of nanoscale and microscale textured Al₂O₃/TiC ceramic tools in dry cutting of hardened steel. *International Journal of Refractory Metals and Hard Materials* 2014;43(0):46-58.
- (6) Kawasegi N, Sugimori H, Morimoto H, Morita N, Hori I. Development of cutting tools with microscale and nanoscale textures to improve frictional behavior. *Precision Engineering* 2009;33(3):248-254.
- (7) Obikawa T, Kamio A, Takaoka H, Osada A. Micro-texture at the coated tool face for high performance cutting. *International Journal of Machine Tools and Manufacture* 2011;51(12):966-972.
- (8) Ze W, Jianxin D, Yang C, Youqiang X, Jun Z. Performance of the self-lubricating textured tools in dry cutting of Ti-6Al-4V. *Int J Adv Manuf Technol* 2012 2012/10/01;62(9-12):943-951.
- (9) Wu Z, Deng J, Su C, Luo C, Xia D. Performance of the micro-texture self-lubricating and pulsating heat pipe self-cooling tools in dry cutting process. *International Journal of Refractory Metals and Hard Materials* 2014.

- (10) Xie J, Luo MJ, Wu KK, Yang LF, Li DH. Experimental study on cutting temperature and cutting force in dry turning of titanium alloy using a non-coated micro-grooved tool. *International Journal of Machine Tools and Manufacture* 2013;73(0):25-36.
- (11) Lian Y, Deng J, Yan G, Cheng H, Zhao J. Preparation of tungsten disulfide (WS₂) soft-coated nano-textured self-lubricating tool and its cutting performance. *Int J Adv Manuf Technol* 2013 2013/10/01;68(9-12):2033-2042.
- (12) Sugihara T, Enomoto T. Crater and flank wear resistance of cutting tools having micro textured surfaces. *Precision Engineering* 2013;37(4):888-896.
- (13) Xing Y, Deng J, Zhang K, Zhang G, Gao H. Effect of femtosecond laser pretreatment on wear resistance of Al₂O₃/TiC ceramic tools in dry cutting. *International Journal of Refractory Metals and Hard Materials* 2014;43(0):291-301.
- (14) Sugihara T, Enomoto T. Improving anti-adhesion in aluminum alloy cutting by micro stripe texture. *Precision Engineering* 2012;36(2):229-237.
- (15) Fatima A, Mativenga P. Assessment of tool rake surface structure geometry for enhanced contact phenomena. *Int J Adv Manuf Technol* 2013 2013/05/29:1-6.
- (16) Fatima A, Mativenga PT. Performance of flank face structured cutting tools in machining of AISI/SAE 4140 over a range of cutting speeds. *Proceedings of the Institution of Mechanical Engineers, Part B: Journal of Engineering Manufacture* 2014 November 10, 2014.
- (17) Shu LH, Ueda K, Chiu I, Cheong H. Biologically inspired design. *CIRP Annals - Manufacturing Technology* 2011;60(2):673-693.
- (18) Wu JH, Phillips BS, Jiang W, Sanders JH, Zabinski JS, Malshe AP. Bio-inspired surface engineering and tribology of MoS₂ overcoated cBN-TiN composite coating. *Wear* 2006;261(5-6):592-599.
- (19) Tong J, Zhang Z, Ma Y, Chen D, Jia B, Menon C. Abrasive wear of embossed surfaces with convex domes. *Wear* 2012;274-275(0):196-202.
- (20) Bio-replicated forming of the biomimetic drag-reducing surface based on underwater low-resistance scarfskins. *Mechatronics and Automation (ICMA), 2010 International Conference on*; 4-7 Aug. 2010; ; 2010.
- (21) Abdel-Aal HA, Mansori ME. Reptilian Skin as a Biomimetic Analogue for the Design of Deterministic Tribosurfaces. In: Gruber P, Bruckner D, Hellmich C, Schmiedmayer H, Stachelberger H, Gebeshuber IC, editors. *Biomimetics -- Materials, Structures and Processes*: Springer Berlin Heidelberg; 2011. p. 51-79; 4.
- (22) Fatima A, Whitehead DJ, Mativenga PT. Femtosecond laser surface structuring of carbide tooling for modifying contact phenomena. *Proceedings of the Institution of Mechanical Engineers, Part B: Journal of Engineering Manufacture* 2014 January 23, 2014;vol. 228(11):1325-1337.

(23) Fatima A, Mativenga PT. A review of tool–chip contact length models in machining and future direction for improvement. Proceedings of the Institution of Mechanical Engineers, Part B: Journal of Engineering Manufacture 2013 March 1, 2013;227(3):345-356.

(24) Determining the effect of interface friction on tool-chip contact length in orthogonal cutting using the finite element method. MATADOR-07.

(25) Balogun VA, Mativenga PT. Modelling of direct energy requirements in mechanical machining processes. Journal of Cleaner Production 2013;41(0):179-186.

(26) Iqbal SA, Mativenga PT, Sheikh MA. Characterization of machining of AISI 1045 steel over a wide range of cutting speeds. Part 1: Investigation of contact phenomena. Proceedings of the Institution of Mechanical Engineers, Part B: Journal of Engineering Manufacture 2007 May 1, 2007;221(5):909-916.

(27) Fahad M, Mativenga PT, Sheikh MA. An investigation of multilayer coated (TiCN/Al₂O₃-TiN) tungsten carbide tools in high speed cutting using a hybrid finite element and experimental technique. Proceedings of the Institution of Mechanical Engineers, Part B: Journal of Engineering Manufacture 2011 October 1, 2011;225(10):1835-1850.

(28) Akbar F, Mativenga PT, Sheikh MA. An evaluation of heat partition in the high-speed turning of AISI/SAE 4140 steel with uncoated and TiN-coated tools. Proceedings of the Institution of Mechanical Engineers, Part B: Journal of Engineering Manufacture 2008 July 1, 2008;222(7):759-771.